Int. J. Electrochem. Sci., 15 **(2020)** 5049 – 5057, doi: 10.20964/2020.06.79

International Journal of
ELECTROCHEMICAL
SCIENCE
www.electrochemsci.org

Short Communication

Electrochemical Detection of Ascorbic Acid in Citrus Juices using Mn-doped ZnO nanorods modified graphene oxide

Lu Zhang

Department of Life Science, Lvliang University, Lvliang 033000, China
E-mail: Luzhang1663@sina.com

Received: 8 February 2020 / *Accepted:* 30 March 2020 / *Published:* 10 May 2020

Modified graphene oxide (GO) electrochemical sensor was successfully used to determine ascorbic acid (AA). Manganese (Mn)-doped ZnO nanorods (ZnO NRs) was synthesized through the electrochemical technique and applied for modification of GO/glassy carbon electrode (GCE). Field emission scanning electron microscopy and X-ray diffraction analysis were applied to characterize the morphological and structural properties of synthesized Mn-doped ZnO NRs. Cyclic voltammetry and differential pulse voltammetry analysis were used to electrochemically sensing the properties of Mn-doped ZnO NRs/GO/GCE. The electrochemical studies exhibited the modified electrode had fast response, selective and stable in determining AA. The sensitivity and detection limit of sensor were estimated 0.169 $\mu AmM^{-1}cm^2$, 0.02 µM, respectively. The sensor response was studied to determine AA content in orange juice as real sample.

Keywords: Mn-doped ZnO nanorods; Ascorbic acid electrochemical sensor; Graphene oxide; Cyclic voltammetry; Differential pulse voltammetry

1. INTRODUCTION

Plant and animal tissues contain ascorbic acid (AA) that play a vital role in several biological reactions like inhibiting and freeing from cancer and scavenging free radicals [1, 2]. AA encourages resistance against oxidative stress due to its antioxidant nature [3]. It is seen as an important vitamin because of its antioxidant and p regulating attributes [4]. Medical researches state that AA can treat colds, infertility, AIDS, cancer, and even mental disorders [5, 6].

Conventional methods for AA assessment include titration by an oxidant solution: bromate, potassium iodate or dichlorophenol indophenol [7]. Chromatographic techniques has shown to be a sensitive and selective method for AA evaluation in biological fluids and foodstuffs [8]. UV-vis absorbance-based determinations and Fluorimetric techniques were also carried out for AA detection [9, 10]. The major drawbacks of these methods are that they are arduous and requires expensive or rare

reagents. Some methods still have errors in the steps of manipulation. Hence there is a demand to come up with a non-complex, highly sensitive method with reliability and accuracy [11]. Of the mentioned methods, electrochemical methods are simple, cost-effective and can be miniaturized to detect AA [12, 13].

Modified electrodes using nanostructures that include carbon, gold, and metal oxide nanostructures enables electron transfer of biomolecules in a direct manner. Of the metal oxide nanostructures, Zinc oxide is most suitable to fabricate adept sensors because of their wide band gap (3.37 eV), 60eV excitation binding energy, high electron transfer and their non-toxic behavior [14].

Graphene is a single planar sheet of one atom thickness comprising of carbon atoms of sp^2 hybridization arranged in a honeycomb lattice [15]. In the light of recent years, graphene has grasped attention because of its highly mobile charge carriers, better specific surface area, and superior electrical conductivity [16]. So, nanostructures based on graphene like zinc oxide/graphene can be explored further as novel materials to be employed as modified electrodes for improving the sensitivity of the sensor.

As far as we know, no scientific research has been published yet to determine AA by employing zinc oxide nanorods / graphene oxide (GO) electrodes. In the current work, we bring forward the fabrication and application of a modified graphene oxide electrode based on Manganese doped ZnO NRs to determine ascorbic acid. X-ray diffraction (XRD) and field emission scanning electron microscopy (FESEM) analyses were applied in the structural characterization of the prepared samples. Cyclic voltammetry and differential pulse voltammetry measurements were used to consider the electrochemical characterization of the sensors.

2. MATERIALS AND METHOD

Graphene oxide modified glassy carbon electrode (GO/GCE) was made by drop-casting of GO suspensions (1µL) on the surface of cleaned GCEs, and then dried in an oven at 50 °C. Then, ZnO nanostructures were grown by two electrode electrochemical Teflon cell and the aqueous solution inside the cell was heated by a hot plate heater. 25 mM of zinc nitrate hydrate ($Zn(NO_3)_26H_2O$, 99.99%) and 25 mM of hexamethylenetetramine (HMT; $C_6H_{12}N_4$, 99%) were dissolved in DI water (50 ml) under magnetic stirring to form the solution for nanorods growth. For the experimental synthesis of Mn-doped ZnO, 1 M HMT, 1 M Zinc acetate dihydrate and manganese tetrachloride with concentration of 5 M were dissolved individually in 25 ml DI water respectively. Ammonia was added to the solution for pH adjustment to 10 and is mixed for 3h. This solution was poured into the galvanic cell. The Pt electrode as the anode and GO/GCE as the cathode were placed inside the galvanic cell. ZnO nanorods grown in vertical alignment was produced with 0.3 mA/cm^2 current density, 95 °C temperature, and one hour growth time. The samples were washed using DI water and dried by N_2 gas.

Field emission scanning electron microscopy (FE-SEM, FEI Sirion 200) was used to investigate the morphology of the synthesized ZnO nanostructure. An energy-dispersive X-ray (EDX) spectrometry was used to examine the detailed elemental analysis of the samples. The structural characteristic of the sample was studied using X-ray Diffractometer (XRD) (D8 Focus, Bruker, Germany). Electrochemical impedance spectroscopy (EIS) was used to examine the charge transfer and recombination processes

with a potential of 10 mV at frequencies range from 0.1 Hz to 0.1MHz. Cyclic voltammetry (CV) measurements were done in –0.1 to 1 V potential range at a 30 mVs^{-1} scan rate in phosphate buffer at pH 7.4. Commercial orange juice samples were prepared from local grocery stores. 20 mL orange juice were stirred for 20 minutes in a glass vessel. Then, it was cleaned by a syringe filter. Finally, before analysis, the samples were appropriately diluted into the supporting electrolyte.

3. RESULTS AND DISCUSSION

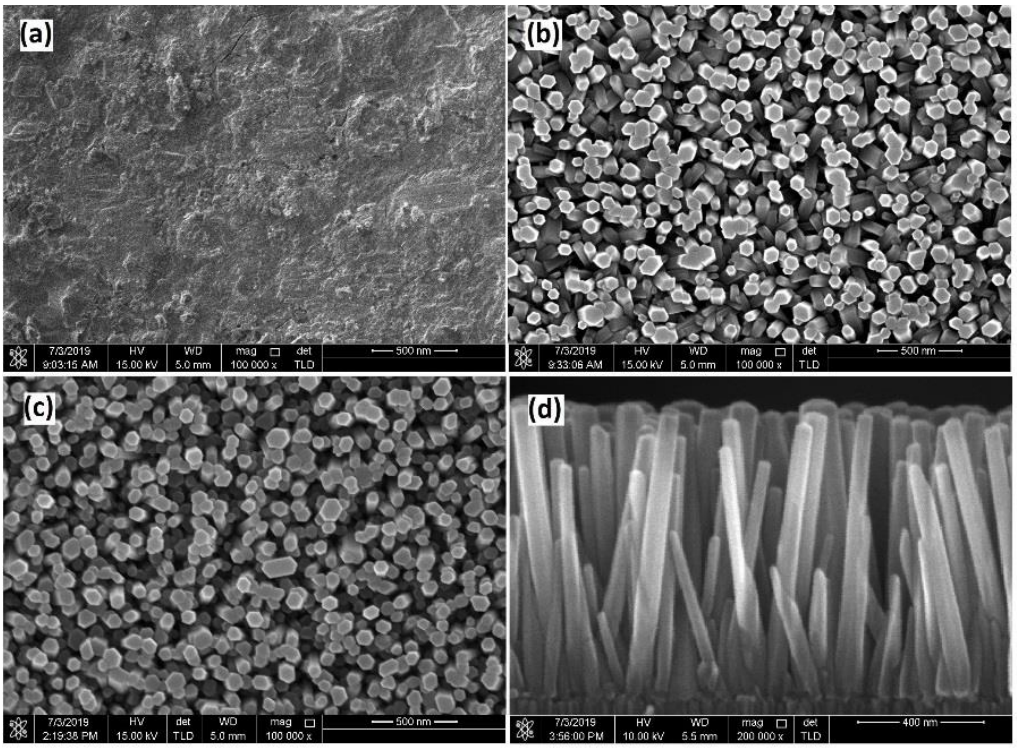

Figure 1. FESEM images of (a) GO/GCE, (b) ZnO NRs/GO/GCE and (c) Top and (d) cross section view of Mn-doped ZnO NRs/GO/GCE electrodes at 95 °C growth temperature and 0.3 mA/cm^2 current density.

A facile chemical method was used to grow highly ordered ZnO nanorods array on the GO/GCE. The uniform growth of ZnO nanorods on the whole GO/GCE substrate surface is shown in FESEM images in Figure 1a. The top surface of the Nanorods seems to have many step edges and the side surface appeared smooth from the top and side views. As seen in Fig. 1a and b, the ZnO nanorods are approximately 60 nm in diameter and 900 nm in length. The nanorods showed the general growth features of crystal-like with hexagonal facets. The ZnO nanorods are vertically aligned on the GO/GCE. Besides, the increase in Mn doping had resulted in variation and an increase of the Nanorods diameter. It is clear that doping of the Mn ions had resulted in the increment of the average height of the ZnO Nanorods (figure 1c and d). The mean diameter and height of the Mn-doped ZnO nanorods were approximately 75 nm and 1.2 μm, respectively. Also, it is understood that adding Mn had resulted in the increment of the diameter of ZnO nanorods, which can be clearly seen in the surface morphologies.

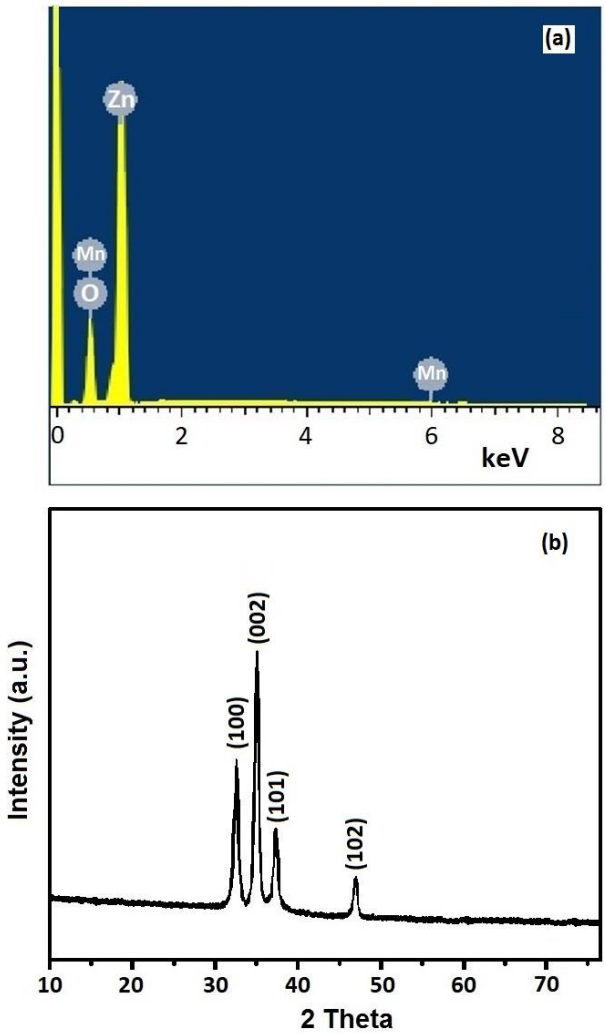

Figure 2. (a) EDAX spectra and (b) XRD pattern of Mn-doped ZnO nanostructures

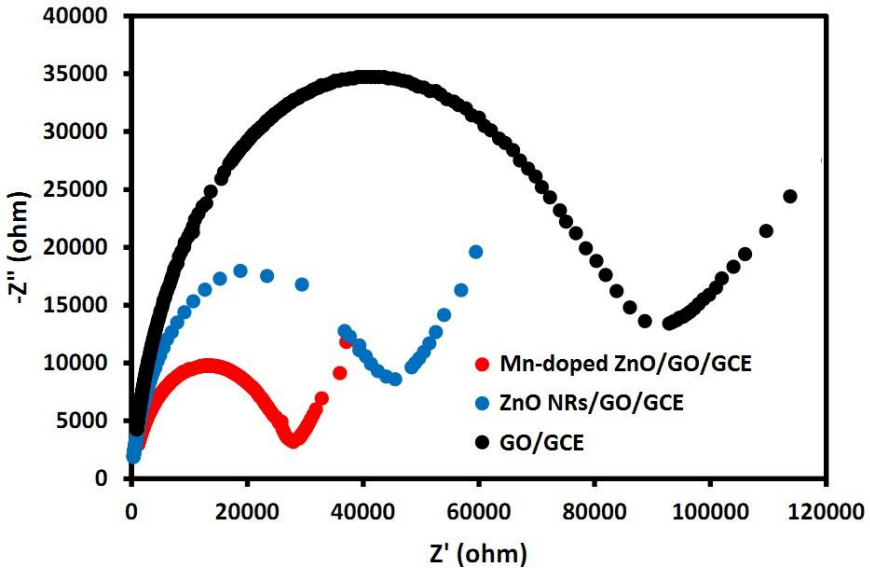

Figure 3. Nyquist plots of GO/GCE, undoped and Mn-doped ZnO NRs/GO/GCE

EDAX spectra of Mn-doped ZnO nanostructures in Fig. 2a detects the existence of elements in the sample. The spectra of Mn-doped ZnO showed peaks with atomic concentrations such as Mn – 3.31%, Zn – 30.53%, and ZnO – 66.16%. Mn substitution in ZnO lattice was found.

Figure 2b exhibits the XRD patterns of the pure and Mn-doped ZnO. The pattern showed only the peaks that can be indexed to hexagonal wurtzite ZnO structure (JCPDS No. 36 - 1451), without secondary peaks from possible impurities like Mn oxides which might indicate the uniform dispersion of Mn in the ZnO matrix [17].

In order to complete the information about the charge transfer efficiency and interface charge separation of Mn-doped ZnO/GO/GCE, the electrochemical impedance measurement was done [18]. Fig. 3 indicates a Nyquist plot between an imaginary and real impedance for ZnO nanorods with Mn doping. The radius of the arc reflects the resistance of interface layer at the surface of the electrode [19]. As the efficiency of the charge transfer decreases, the arc radius increases. Mn doping decreases the interface layer resistances, showing the developed efficiency of charge transfer and interfacial charge-carrier separation on the surface of ZnO. These results prove that doping Mn ions in ZnO nanorods can lead to higher free-electron carriers that accelerate charge transfer and reduces the resistance, it is useful for the sensing activity of ZnO nanorods.

500 µM AA in a 7.4 pH phosphate buffer (PB) solution at bare GO/GCE, ZnO NRs/GO/GCE and Mn-doped ZnO NRs/GO/GCE underwent to obtain cyclic voltammograms at 30 mV/s scan rate and -0.1 to 1.0 V potential range. The sensing was done due to the adsorbance of AA molecules to the surface of the Mn-doped ZnO NRs/GO/GCE. Then hydrolyzation of AA with water and oxidation occurred to get dehydroascorbic acid. Electrons were released during the oxidation process that allowed the detection of current. From figure 4, it is clear that the reduction peak is absent meaning that the AA oxidation process is irreversible [20]. The cyclic voltammograms additionally depicts that higher AA oxidation currents were shown by the Mn-doped ZnO NRs/GO/GCE than the GO/GCE and ZnO NRs/GO/GCE electrodes. The increase in the electro active surface area had enabled the increase of peak current in the Mn-doped ZnO NRs/GO/GCE. The overall potentials were low for all the electrodes for AA oxidation. So, catalytic activity was displayed by all the electrodes for AA oxidation. According to the previous studies, it is understood that doped ZnO NRs/graphene-based electrodes exhibit higher selectivity of AA in the existence of various anlytes [21, 22]. So, the voltammetric sensor to detect AA was fabricated using Mn-doped ZnO NRs/GO/GCE.

To detect AA, a voltammetric sensor with a differential pulse voltammetry (DPV) was fabricated. The received DPVs for Mn-doped ZnO nanorods/GO/GCE at varying concentrations of AA are shown in figure 5a. The concentration ranged between 0.5 mM to 5.5 mM in a 7.4 pH phosphate buffer solution. The current at the oxidation peak and the concentration of AA were in direct proportion. The calibration graph is plotted for the oxidation peak current vs the AA concentration (figure 5b). The plot had R^2=0.9982, the sensitivity of 0.169 $\mu AmM^{-1}cm^2$, 0.02 µM limit of detection was calculated. The limit of detection was calculated by using a rigorous statistics approach.

A solution of 500 µM AA in 0.1 M phosphate buffer was used to perform DPV analysis of the Mn-doped ZnO NRs/GO/GCE to investigate the reproducibility. 2.02% standard deviation for five different investigations were obtained indicating the reproducibility of the electrode to detect AA.

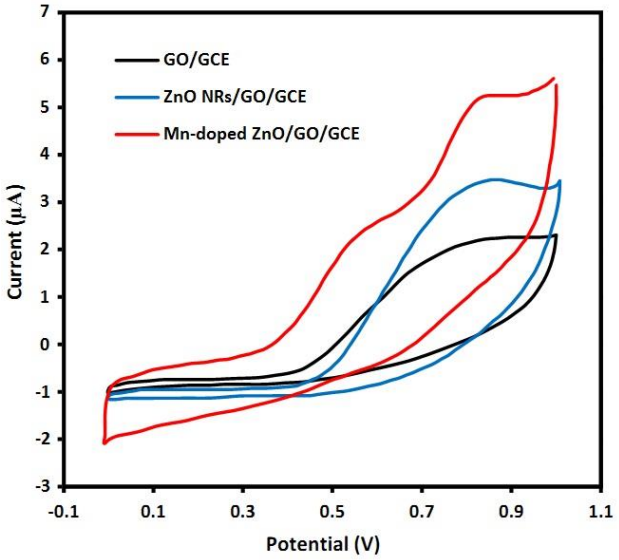

Figure 4. Cyclic voltammetry of unmodified GO/GCE, ZnO NRs/GO/GCE and Mn-doped ZnO nanorods/GO/GCE for 0.5 Mm AA in 0.1 M phosphate buffer at 30 mV/s scan rate.

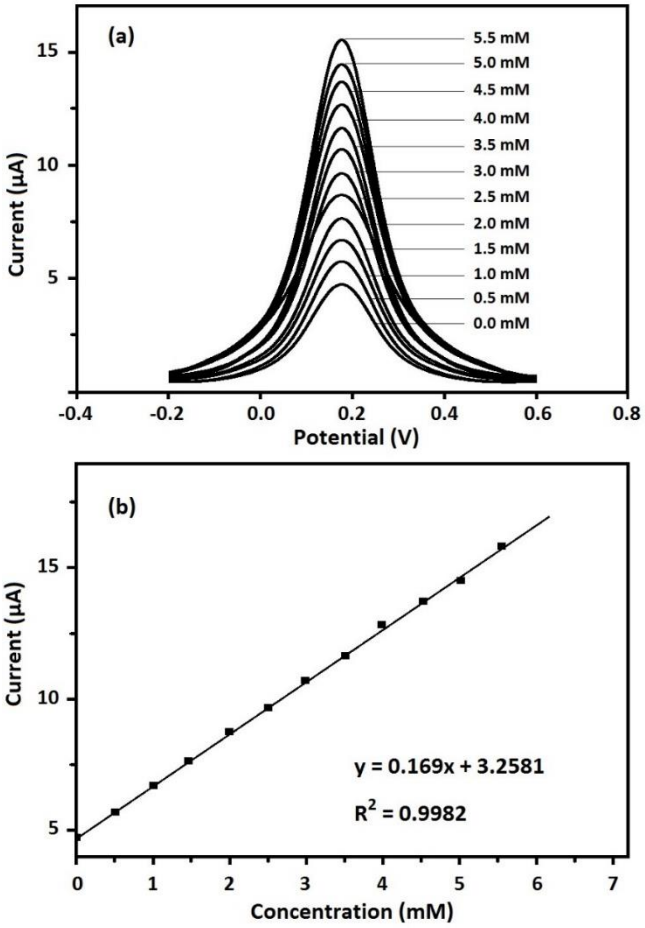

Figure 5. (a) DPV response of Mn-doped ZnO nanorods/GO/GCE electrode (b) Calibration plot of linear variation of DPV peak current in varying concentration of ascorbic acid at 0.1 M phosphate buffer solution and 30 mV s^{-1} scan rate.

The features of different modified electrodes reported in previous studies to detect AA were compared and tabulated in table 1. These results make it clear that the proposed Mn-doped ZnO NRs/GO/GCE sensor is a suitable successor for day to day analysis of AA and can be implemented to determine AA in fruit samples.

Table 1. Comparison of ascorbic acid determination in various samples by electrochemical methods

Electrode	Method	Sensitivity ($\mu AmM^{-1}cm^2$)	Limit of detection (μM)	Ref.
β-CD/rGO/SPE	DPV	-	0.067	[23]
MoS/rGO nanocomposite	DPV	0.12	0.072	[24]
EGNWs	DPV	8.74	1.8	[25]
ANF-C700	DPV	1.06	0.117	[26]
Fe3O4 CNT-C/GCE	SWV	0.49	0.24	[27]
APM/CNTPE	DPV	60.3	0.08	[28]
Mn-doped ZnO NRs/GO/GCE	DPV	0.169	0.02	This work

To promote it as an application tool for analysis, investigation of the Mn-doped ZnO NRs/GO/GCE electrode was done by detecting AA in natural orange juices. These results are tabulated in table 2. The orange juices were mixed in 7.4 pH 0.1 M phosphate buffer solution and a known concentration of AA was added to it. The recovery of detection values of AA for three samples were in the range of 98.2–116%. Satisfactory RSD and recovery were obtained signifying that the proposed sensor has upright accuracy. Thus, the prospective Mn-doped ZnO nanorods/GO/GCE electrochemical sensor was appropriate to determine the AA in real samples.

Table 2. Results obtained at AA determination in orange juices by DPV

Samples	Content (μMl^{-1})	Added concentration (μMl^{-1})	Found concentration (μMl^{-1})	Recovery (%)	RSD (%)
1	10.0	15.0	25.5	102.0	3.1
2	15.0	15.0	31.6	98.2	3.6
3	11.5	15.0	28.1	116.0	2.9

4. CONCLUSIONS

The Electrochemical characterization of Mn-doped ZnO NRs/GO/GCE electrode for the determination of AA was performed by CV and DPV techniques. The Mn-doped ZnO NRs were synthesized through a facile electrochemical method and used for modification of GO/GCE. The structural properties of synthesized Mn-doped ZnO NRs were studied by FESEM and XRD analyses. The results of the structural studies showed that high aspect ratio of Mn-doped ZnO NRs were

synthesized in hexagonal wurtzite structure. The CV studies of the Mn-doped ZnO NRs/GO/GCE showed a sharp and stable oxidation peak in a 0.83 V of AA. The DPV results showed that Mn-doped ZnO NRs/GO/GCE was fast response, sensitive, selective and stable in the determination of AA. The sensitivity and detection limit of sensor were estimated 0.169 $\mu AmM^{-1}cm^2$ and 0.02 µM, respectively. The results showed that the modified electrode was successfully applied to AA detection in orange juice as a real sample.

References

1. N. Smirnoff, *Free Radical Biology and Medicine*, 122 (2018) 116.
2. R. Dalvand, S. Mahmud and J. Rouhi, *Materials Letters*, 160 (2015) 444.
3. J. Guil-Guerrero, *Quaternary Science Reviews*, 157 (2017) 176.
4. B. Han, X. Duan, Y. Wang, K. Zhu, J. Zhang, R. Wang, H. Hu, F. Qi, J. Pan and Y. Yan, *Scientific reports*, 7 (2017) 46185.
5. S.-j. Kim, Y.K. Cho, C. Lee, M.H. Kim and Y. Lee, *Biosensors and Bioelectronics*, 77 (2016) 1144.
6. F. Husairi, J. Rouhi, K. Eswar, C.R. Ooi, M. Rusop and S. Abdullah, *Sensors and Actuators A: Physical*, 236 (2015) 11.
7. A.O. Patrick, U.A. Fabian, I.C. Peace and O.O. Fred, *Journal of Environmental Science, Toxicology and Food Technology*, 10 (2016) 17.
8. F.R. Najwa and A. Azrina, *International Food Research Journal*, 24 (2017) 726.
9. H. Bi, A.C. Fernandes, S. Cardoso and P. Freitas, *Sensors and Actuators B: Chemical*, 224 (2016) 668.
10. N. Hassanzadeh and H.R. Zare-Mehrjardi, *International Journal of Electrochemical Science*, 12 (2017) 3950.
11. S. Qi, B. Zhao, H. Tang and X. Jiang, *Electrochimica Acta*, 161 (2015) 395.
12. C. Xu, B. Liu, W. Ning and X. Wang, *International Journal of Electrochemical Science*, 14 (2019) 1670.
13. J. Rouhi, S. Mahmud, S.D. Hutagalung and S. Kakooei, *Journal of Micro/Nanolithography, MEMS, and MOEMS*, 10 (2011) 043002.
14. R. Dalvand, S. Mahmud, J. Rouhi and C.R. Ooi, *Materials Letters*, 146 (2015) 65.
15. S. Changaei, J. Zamir-Anvari, N.-S. Heydari, S.G. Zamharir, M. Arshadi, B. Bahrami, J. Rouhi and R. Karimzadeh, *Journal of Electronic Materials*, 48 (2019) 6216.
16. J.D. Cox, I. Silveiro and F.J. García de Abajo, *ACS nano*, 10 (2016) 1995.
17. M. Sharma, R. Gayen, A. Pal, D. Kanjilal and R. Chatterjee, *Journal of alloys and compounds*, 509 (2011) 7259.
18. J. Rouhi, S. Mahmud, N. Naderi, C.R. Ooi and M.R. Mahmood, *Nanoscale research letters*, 8 (2013) 1.
19. H. Zhu and G. Xu, *International Journal of Electrochemical Science*, 12 (2017) 3873.
20. N. Dhanalakshmi, T. Priya, V. Karthikeyan and N. Thinakaran, *Journal of pharmaceutical and biomedical analysis*, 174 (2019) 182.
21. X. Chen, G. Zhang, L. Shi, S. Pan, W. Liu and H. Pan, *Materials Science and Engineering: C*, 65 (2016) 80.
22. Q. Wang, H. Yue, J. Zhang, X. Gao, H. Zhang, X. Lin, B. Wang and D. Bychanok, *Ionics*, 24 (2018) 2499.
23. Q. Qin, X. Bai and Z. Hua, *Journal of Electroanalytical Chemistry*, 782 (2016) 50.
24. L. Xing and Z. Ma, *Microchimica Acta*, 183 (2016) 257.

25. P.K. Roy, A. Ganguly, W.-H. Yang, C.-T. Wu, J.-S. Hwang, Y. Tai, K.-H. Chen, L.-C. Chen and S. Chattopadhyay, *Biosensors and Bioelectronics*, 70 (2015) 137.
26. M. Taleb, R. Ivanov, S. Bereznev, S.H. Kazemi and I. Hussainova, *Microchimica Acta*, 184 (2017) 897.
27. D.M. Fernandes, M. Costa, C. Pereira, B. Bachiller-Baeza, I. Rodríguez-Ramos, A. Guerrero-Ruiz and C. Freire, *Journal of colloid and interface science*, 432 (2014) 207.
28. S. Gheibi, H. Karimi-Maleh, M.A. Khalilzadeh and H. Bagheri, *Journal of Food Science and Technology*, 52 (2015) 276.